

A Qubit-Efficient Variational Selected Configuration-Interaction Method

Daniel Yoffe^{1,2}, Amir Natan¹ and Adi Makmal^{2,3}

¹Department of Physical Electronics, Tel Aviv University, 69978 Tel Aviv, Israel.

²The Engineering Faculty, Bar-Ilan University, 52900 Ramat-Gan, Israel.

³The center for Quantum Entanglement Science and Technology, Bar-Ilan University, 52900 Ramat-Gan, Israel.

Contributing authors: d4444i@gmail.com; amirnatan@tauex.tau.ac.il;
adi.makmal@biu.ac.il;

Abstract

Finding the ground-state energy of molecules is an important and challenging computational problem for which quantum computing can potentially find efficient solutions. The variational quantum eigensolver (VQE) is a quantum algorithm that tackles the molecular ground-state problem and is regarded as one of the flagships of quantum computing. Yet, to date, only very small molecules were computed via VQE, due to high noise levels in current quantum devices. Here we present an alternative variational quantum scheme that requires significantly less qubits. The reduction in qubit number allows for shallower circuits to be sufficient, rendering the method more resistant to noise. The proposed algorithm, termed variational quantum selected-configuration-interaction (VQ-SCI), is based on: (a) representing the target groundstate as a superposition of Slater determinant configurations, encoded directly upon the quantum computational basis states; and (b) selecting *a-priori* only the most dominant configurations. This is demonstrated through a set of groundstate calculations of the H_2 , LiH , BeH_2 , H_2O , NH_3 and C_2H_4 molecules in the sto-3g basis set, performed on IBM quantum devices. We show that the VQ-SCI reaches the full-CI (FCI) energy within chemical accuracy using the lowest number of qubits reported to date. Moreover, when the SCI matrix is generated “on the fly”, the VQ-SCI requires exponentially less memory than classical SCI methods. This offers a potential remedy to a severe memory bottleneck problem in classical SCI calculations. Finally, the proposed scheme is general and can be straightforwardly applied for finding the groundstate of any Hermitian matrix, outside the chemical context.

Keywords: variational quantum algorithms, variational quantum eigensolver, qubit-efficient, electronic structure, configuration interaction, first quantization

1 Introduction

Finding the electronic structure of a chemical system is at the heart of computational chemistry with countless applications in material design, drug design, and scientific research [1–5]. This requires the solution of the non-relativistic time-independent Schrödinger equation:

$$\mathcal{H}|\Psi\rangle = \mathcal{E}|\Psi\rangle, \quad (1)$$

where \mathcal{H} is the system’s Hamiltonian, \mathcal{E} is the total energy, and Ψ is the corresponding groundstate, dictating the electronic structure of the system. However, solving the electronic Schrödinger equation directly is difficult because of the enormous dimensionality of the problem, which grows rapidly with the number of electrons. As relatively small molecules already encapsulate tens of electrons, e.g., water ($N=10$) or benzene ($N=42$), finding an exact solution becomes intractable, even for very strong classical computers [6].

The variational quantum eigensolver (VQE) is a recent quantum algorithm that aims at solving the electronic structure problem in polynomial timescales [7–9]. It is based on a parameterized quantum circuit that is tuned iteratively until a minimum energy value is attained. The central advantage of VQE, in comparison to previous quantum algorithms (e.g. phase-estimation [10, 11]), is that it requires shallower circuits which are more noise tolerant. It is therefore better suited for the current noisy intermediate scale quantum (NISQ) devices and is considered to be a prime candidate for demonstrating quantum advantage.

Yet, despite its promise, VQE has reached only limited success so far. Real quantum hardware VQE demonstrations are still scarce, addressing only small molecules, and reaching insufficient accuracy even for the minimal basis set, see [7, 12–18] for central examples. Moreover, it was estimated that for practical usage VQE would require millions of two-qubit gates and hundreds of *logical*, error-free, qubits [19], much beyond current capabilities. The reason is that VQE in the standard Jordan-Wigner (JW) mapping [20], requires a number of qubits that equals the number of spin-orbitals (M) in a given basis set (assuming no core orbital freezing and symmetry reductions, see below for a formal description), which grows with the system. As the number of qubits increases, more gates are required for the variational circuits, which despite being relatively shallow, still accumulate too much noise. Furthermore, even on noiseless simulations, VQE could so far address only small molecules [16, 19, 21] due to its large qubits consumption, which is difficult to simulate.

Several attempts have been made to improve the VQE through computational resource saving and better noise mitigation [8, 22]. For example, some

suggestions have been made to reduce circuit’s depth by replacing the original chemically inspired Ansatz with more heuristic approaches, see e.g. [14, 23–25], which are often prone to particle number and spin symmetry violation. In addition, several attempts to employ better basis sets have been made [18, 26] which led to a more accurate description of the Hamiltonian, thus reaching better accuracy at a comparable computational cost. Reducing the number of distinct Pauli strings required to be measured was also pursued in [14, 27, 28].

Resource saving via qubit reduction was also explored, for example through core orbital freezing (COF) [18, 29], which, however, introduces an uncontrolled approximation. An alternative direction towards qubit reduction, which is also the one we explored, employs a different information encoding, as described next.

Information encoding

The computational resources required for calculating molecular systems are usually measured in terms of the number of electrons in the system, N , and the size of the basis-set, namely the number of spin-orbitals that are taken into account, M . VQE is formulated within the framework of second quantization [22], where each Slater determinant is encoded as a binary string of spin-orbital occupations (see Sec. 2). Accordingly, in the standard JW encoding [20] the quantum state of each qubit encodes the occupation of the corresponding spin-orbital, therefore requiring M qubits, one per spin-orbital. Several studies aimed at reducing this qubit requirement by relying on symmetry considerations, e.g. Z_2 -symmetry based qubit tapering [30] and qubit reduction through molecular point group symmetry [31]. Another attempt was explored in the form of “entanglement forging” [29], where a system of $2N$ qubits is regarded as two, weakly entangled, N qubit systems, thus effectively cutting the number of qubits by half, at a cost of additional classical calculations. Alternatively, when working in the framework of first quantization, other types of encoding may be useful. For example, in the early work of Abrams and Lloyd [10] it was suggested to simulate a chemical system using $N \log M$ qubits, by encoding the spin-orbital of each electron as a separate binary string of length $\log M$. This encoding was later explored in [32], see also [9].

A different encoding associates the k ’th Slater determinant with the computational state $|bin(k)\rangle$, where $bin(k)$ is a predefined decimal-to-binary mapping of k . Such an encoding, denoted *amplitude encoding* in the quantum machine learning literature where it is often used, see [33], or simply *binary encoding*, fully utilizes the capacity of q qubits to encode 2^q amplitudes and is therefore economical in the number of required qubits. Examples for using it in the chemical context include quantum simulation [30, 34, 35], simulating molecular vibrations of a bosonic operator [36], d -level quantum operator (qudits) encodings [37], and finding deuteron ground-state energy [38].

A recent paper suggested using such a binary encoding for finding the molecular groundstate [39] within the variational quantum paradigm. Essentially, this amounts to solving the molecular groundstate problem in the

representation of Slater determinants rather than that of spin-orbital occupations. It enables a FCI calculation with $\log D_{FCI}$ qubits, where $D_{FCI} = \binom{M}{N}$ is the number of Slater determinants that can be composed within a given basis-set. Note that $D_{FCI} = \binom{M/2}{N/2}^2$ when the calculation is spin restricted to equal number of spin up and down electrons $N_{\uparrow} = N_{\downarrow}$ (but without imposing the same spatial orbital for spin up and spin down). In this paper, we use such a spin-restriction assumption, for all the presented analyses.

For a fixed number of electrons and increasing number of spin-orbital candidates, this encoding requires a number of qubits that scales only logarithmically with the number of spin-orbitals, providing an exponential qubit saving over the standard VQE formalism. Indeed, it was demonstrated in [39] that H_2 could be solved to high accuracy with the 6-31G basis set using merely 4 qubits rather than 8, when solved in the basis of Slater determinants. An additional, more qualitative advantage of this scheme is that it leads, by construction, to groundstates that preserve spin and electron number, irrespective of the quantum circuit’s Ansatz, thus allowing the usage of hardware-efficient Ansatz with no computational artifacts, as described in [39].

The problem, however, with performing such a variational quantum FCI calculation directly in the basis of Slater determinants is that it requires using all Slater determinants to encode the Hamiltonian and therefore the measurement of $\mathcal{O}(D_{FCI}^2)$ distinct Pauli strings (see [39] and Sec. 5). This exerts strict limitations on the practical usage of such an approach to (yet again) small molecules. Moreover, the saving in qubit number is mild. For example, the ethylene molecule (C_2H_4 , $N = 16$ electrons) has $M = 28$ spin-orbitals in the minimal sto-3g basis set, hence requiring $\lceil \log_2 D_{FCI} \rceil = \lceil \log_2 \binom{14}{8} \binom{14}{8} \rceil = 24$ qubits, even under spin-restriction, compared to $M = 28$ qubits in the standard VQE. For such a calculation to be feasible the number of Slater determinants that take part in the calculation must therefore be significantly reduced.

Full vs. selected-CI

One way to reduce the number of Slater determinants is to perform a selected-CI (SCI) computation [40]. In this case, the computation is performed on a selected, smaller set, of Slater determinants, instead of the full one, thereby requiring much smaller, yet sparse, matrices to be diagonalized, significantly reducing the computational cost. The SCI scheme has been studied extensively as a classical computational method for half a century, see e.g., [41–45] for some of the first studies that developed heuristics for selecting the best k Slater determinants candidates. They showed that chemical accuracy can be reached with a relatively small subset of Slater determinants, when selected wisely. In recent years, substantial progress has been made with a wide variety of new methods for selecting the most important Slater determinants, using advanced tools from various approaches, e.g., localized orbitals [46], perturbation theory [47], energy cut-off [48], heat-bath sampling approach [49], approximating the amplitudes of the ground-state wavefunction [50], iterative selection [51], and machine learning [52, 53]. These developments led to more scalable and

accurate results, making the classical SCI method a competitive approach for conducting electronic structure calculations with low computational costs. A recent study [54] even considered the usage of a classically computed SCI wavefunction as a target wavefunction for better preparing an initial Ansatz for the ADAPT-VQE scheme [23].

Performing a SCI calculation by means of quantum computing was not yet sufficiently explored. Moreover, executing SCI within the VQE approach, namely constraining the VQE calculation to *any* desirable subset of Slater determinants, is not straightforward. It is possible to constraint the VQE to a specific set of excitations, using a chemically inspired Ansatz, see e.g. [16], but this requires a deep circuit, which accumulates much noise.

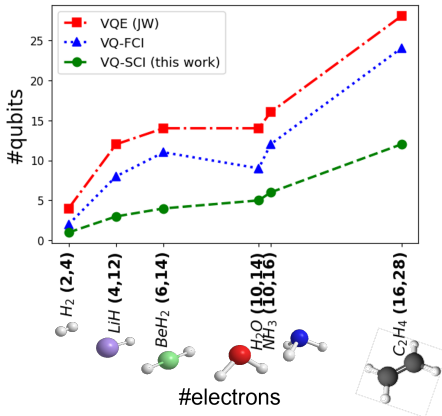


Fig. 1: The number of qubits required to perform groundstate energy calculations of the molecules studied in this paper, ordered by their number of electrons (the NH₃ molecule is slightly shifted for clarity), in the sto-3g basis set, per method. The number of electrons and spin-orbitals (N , M) are written next to each molecule. VQE assumes JW encoding (red squares), VQ-FCI employs all possible Slater determinants (blue triangles), and the proposed VQ-SCI (green circles) employs a small subset of the most significant Slater determinants that lead to the FCI accuracy level, see details in text. The VQ-SCI is shown to be the most economical in the number of required qubits.

1.1 Our approach

Here we develop and explore the idea of solving the electronic structure problem with the aid of quantum computers, by performing variational quantum selected-configuration-interaction (VQ-SCI) calculation, directly in the basis of Slater determinants.

Building upon classical SCI schemes, we perform the selection of k significant Slater determinants classically, but use quantum computers to find the groundstate of the corresponding SCI matrix. By performing the calculation in the Slater determinants basis and encoding the Slater determinants to qubits via a decimal-to-binary encoding, our VQ-SCI method is very modest in qubit consumption. This allows us to perform groundstate energy calculations for

a set of small to medium-size molecules, within the sto-3g basis set, with the smallest number of qubits reported to date, while addressing all electrons in the system and without resorting to any kind of orbital freezing. In particular, we calculated the groundstate of the following molecules: H_2 ($N = 2, M = 4, q = 1$ qubit), LiH ($N = 4, M = 12, q = 3$ qubits), BeH_2 ($N = 6, M = 14, q = 4$ qubits), H_2O ($N = 10, M = 14, q = 5$ qubits), NH_3 ($N = 10, M = 16, q = 6$ qubits), and C_2H_4 ($N = 16, M = 28, q = 12$ qubits), where q is the number of qubits required by VQ-SCI to reach the FCI groundstate energy within chemical accuracy.

To demonstrate the saving in qubits number, Fig. 1 presents the number of qubits required by standard VQE in the JW encoding (red squares) and by our VQ-SCI approach (green circles). For completeness, the number of qubits required by a VQ-FCI method (blue triangles), i.e. when using *all* Slater determinants (similar to the calculations presented in [39]), is also depicted. The figure presents all the molecules we addressed in this paper, ordered by their number of electrons. In all cases the sto-3g basis set is considered and no core orbital freezing is assumed. For the VQE scheme in the JW encoding, M qubits are needed for M spin-orbitals. The VQ-FCI requires $\log(D_{FCI})$, where $D_{FCI} = \binom{M/2}{N/2}^2$ is the number of possible Slater determinants. Finally, our proposed VQ-SCI requires $\log(D_{SCI})$ qubits, where D_{SCI} is the number of significant Slater determinants required to reach the FCI groundstate energy within chemical accuracy. The exact value of D_{SCI} depends on the chosen selection procedure. The one we employed is described in Sec. 4 and reaches $D_{SCI} \approx \sqrt{D_{FCI}}$, thus cutting the number of qubits approximately by half (often more). For both VQ-FCI and VQ-SCI we assumed spin-restriction, as described above. It is seen that while VQ-FCI improves the number of qubits only mildly in comparison to standard VQE, the VQ-SCI requires much fewer qubits and increases much slower than the VQE. Evidently, it requires a number of qubits that is always below the number of electrons in the molecule.

Consequent advantages of the VQ-SCI method in comparison to VQE are: (a) The use of fewer qubits makes shallower circuits sufficient, which translates to a significant reduction in the circuit’s noise. This, in turn, leads to better accuracy; (b) The groundstate Ansatz is constructed as a linear combination of only physical states, which leads to the conservation of total particle number and spin-symmetry, by construction; (c) Selecting the Slater determinants does not come at the cost of using deep chemical inspired circuit Ansätze; and (d) Although the method selects a specific set of Slater determinants, it does not perform any sort of orbital “freezing”. This ability to choose the Slater determinants without being restricted to a specific set of orbitals gives the VQ-SCI method more degrees of freedom, which allow it to include excitations that are often dismissed. These advantages come at the cost of more Pauli strings needed to be measured. We analyze this cost, point to cases where the number of Pauli strings in VQE is nevertheless larger than in the VQ-SCI method, and discuss different directions to reduce it.

Most importantly, the proposed method constitutes a general procedure for finding the lowest eigenvalue and groundstate of a D by D Hermitian matrix, using $\log D$ qubits. In fact, we are only constrained to matrices whose lowest eigenvalue is real (but are not necessarily Hermitian). The scheme can therefore be applied outside the chemical context, for example, in graph theory, where the smallest eigenvalue of the adjacency matrix entails important information on the graph’s structure [55]. Our analysis indicates that in comparison to common classical approaches, the quantum scheme scales similarly with time and logarithmic in memory. This advantage can be achieved only when the calculation is performed on actual quantum hardware and can not be reproduced via classical simulations.

The paper is structured as follows: Sec. 2 describes the necessary background of computational chemistry and the variational quantum eigensolver (VQE) algorithm; Sec. 3 explains the formalism of the proposed VQ-SCI approach, including a detailed example for the case of H_2 ; Sec. 4 presents our computational VQ-SCI results, displaying groundstate energy calculations for H_2 , LiH, BeH_2 , H_2O , NH_3 , and C_2H_4 in the sto-3g basis set, through noiseless, noisy, and real-hardware calculations. Sec. 5 offers a crude resource analysis of the VQ-SCI method and discusses its potential applicability. Sec. 6 concludes the paper and points to future research directions.

2 Background

2.1 Classical computational chemistry

The Hamiltonian of a molecular system of A atoms with N electrons takes the following form (under the Born-Oppenheimer approximation) [1, 2]:

$$\mathcal{H} = \sum_{j=1}^N T_j + \sum_{a=1}^A \sum_{j=1}^N V_{a,j}^{ext} + \sum_{\substack{j=1, \\ k>j}}^N V_{j,k}^{e-e}, \quad (2)$$

where $T_j = -\frac{\nabla_j^2}{2}$ is the kinetic energy of a single electron, $V_{a,j}^{ext} = -\frac{Z_a}{|\vec{R}_a - \vec{r}_j|}$ is the external electronic nuclei-electron attraction, and $V_{j,k}^{e-e} = \frac{1}{|\vec{r}_j - \vec{r}_k|}$ accounts for the electron-electron interactions. Atomic units are used throughout.

The Hartree-Fock (HF) method provides an approximated solution for finding the groundstate of the Schrödinger Eq. (1) with the molecular Hamiltonian of Eq. (2) in the form of a single Slater determinant wavefunction:

$$\Phi(\vec{s}_1, \dots, \vec{s}_N) = \frac{1}{\sqrt{N!}} \begin{vmatrix} \chi_1(\vec{s}_1) & \chi_2(\vec{s}_1) & \dots & \chi_N(\vec{s}_1) \\ \chi_1(\vec{s}_2) & \chi_2(\vec{s}_2) & \dots & \chi_N(\vec{s}_2) \\ \vdots & \vdots & \ddots & \vdots \\ \chi_1(\vec{s}_N) & \chi_2(\vec{s}_N) & \dots & \chi_N(\vec{s}_N) \end{vmatrix} \equiv SD\{\chi_1, \dots, \chi_N\} \quad , \quad (3)$$

where $\{\chi_j(\vec{s}_k)\}$ are a set of molecular orbitals, $SD\{\chi_1, \dots, \chi_N\}$ mark the Slater determinant composed of the $\{\chi_1, \dots, \chi_N\}$ molecular orbitals, and \vec{s} stands for the spatial (\vec{r}) and spin (α) coordinates of a single electron. The HF approximation is the simplest, hence most efficient, approximation to an uncorrelated N -electron wavefunction, which satisfies the antisymmetry requirement. Yet, it performs rather poorly, in terms of the achievable groundstate energy.

Configuration interaction (CI)

One way to go beyond the HF approximation is via the configuration-interaction (CI) method, which represents the molecular groundstate as a linear combination of many Slater determinants (rather than just a single one):

$$|\Psi(\vec{s}_1, \dots, \vec{s}_N)\rangle = \sum_k c_k |\Phi_k(\vec{s}_1, \dots, \vec{s}_N)\rangle. \quad (4)$$

It is guaranteed by the variational theorem that taking a larger-size set of Slater determinants (or, synonymously, configurations) necessarily brings us closer to the desired groundstate wavefunction. However, reaching absolute accuracy might well require an intractable large set of Slater determinants. A common way to bound the calculation to a manageable number of Slater determinants is to employ confined basis sets (such as the sto-3g) with finite sets of $M > N$ molecular spin-orbitals, allowing the composition of $F = \binom{M}{N}$ different Slater determinants [56]. When the summation in Eq. 4 accounts for all possible F Slater determinants, we refer to the calculation as a Full-CI (FCI) calculation, whereas when a smaller subset of $D < F$ Slater determinants is employed we refer to the calculation as a Selected-CI (SCI) calculation. In either case, finding the groundstate of a molecule amounts to finding the lowest eigenstate, Ψ_0 , of the following Hermitian matrix:

$$M_{CI}|\Psi_0\rangle = e_0|\Psi_0\rangle, \quad M_{CI}(k, j) = \langle\Phi_k|\mathcal{H}|\Phi_j\rangle, \quad (5)$$

which represents the molecular Hamiltonian operator \mathcal{H} of Eq. 2 in the basis of Slater determinants. Reducing the number of Slater determinants used in the calculation through SCI leads directly to reducing the dimension of the M_{CI} Hamiltonian matrix.

The classical SCI method is a 2-phase algorithm: (I) Select D Slater determinants and construct the D -dimensional SCI matrix in the form of Eq. 5; (II) Find the lowest eigenstate and eigenvalue of the SCI matrix. The second part of the algorithm is the computational bottleneck. It has a naive time complexity of $\mathcal{O}(D^3)$, which can be reduced to $\mathcal{O}(D^2)$ and an $\mathcal{O}(D)$ space complexity using iterative methods, such as the Davidson algorithm [57]. The proposed VQ-SCI method, described in Sec. 3, performs the second phase of the SCI algorithm by means of quantum computing.

2.2 Variational quantum eigensolver (VQE)

The VQE method [7] searches for the system’s groundstate by optimizing a parameterized quantum state $\psi(\theta)$ to minimize the energy expectation value:

$$\Psi_0 = \operatorname{argmin}_{\psi(\theta)} \langle \psi(\theta) | \mathcal{H} | \psi(\theta) \rangle, \quad (6)$$

as dictated by the variational principle. Here the molecular Hamiltonian takes the 2^{nd} quantization form:

$$\mathcal{H} = \sum_{p,q=1}^M h_{pq} a_p^\dagger a_q + \sum_{p,q,r,s=1}^M h_{pqrs} a_p^\dagger a_q^\dagger a_r a_s, \quad (7)$$

where M is the number of spin-orbitals, and a_p^\dagger and a_p are the fermionic creation and annihilation operators, respectively. The scalar coefficients h_{pq} and h_{pqrs} are defined as follows, using the Hamiltonian parts of Eq. 2:

$$\begin{aligned} h_{pq} &= \langle \chi_p | T_q + \sum_{a=1}^A V_{a,q}^{ext} | \chi_q \rangle = \int \chi_p^*(\vec{s}) \left(-\frac{\nabla_r^2}{2} - \sum_{a=1}^A \frac{Z_a}{|\vec{R}_a - \vec{r}|} \right) \chi_q(\vec{s}) d\vec{s} \\ h_{pqrs} &= \langle \chi_p \chi_q | V_{1,2}^{e-e} | \chi_r \chi_s \rangle = \iint \frac{\chi_p^*(\vec{s}_1) \chi_q^*(\vec{s}_2) \chi_r(\vec{s}_2) \chi_s(\vec{s}_1)}{|\vec{r}_1 - \vec{r}_2|} d\vec{s}_1 d\vec{s}_2, \end{aligned} \quad (8)$$

where χ are molecular spin-orbitals of a single electron, as in Eq. 3.

The Hamiltonian of Eq. 7 is encoded to the quantum circuit by mapping each fermionic operator to a string (tensor product) of single-qubit Pauli operators, resulting with the following summation: $\mathcal{H} = \sum_k a_k P_k$, where a_k are constant coefficients and $P_k = \bigotimes_{j=0}^{q-1} \sigma_{i,j}$ are strings of Pauli operators; the $\sigma_{i,j}$ is the i ’th Pauli operator ($i \in \{X, Y, Z, I\}$) applied onto the j ’th qubit, and $q = M$ is the number of qubits in the circuit. Consequently, minimizing Eq. 6 is performed by minimizing over $\sum_k a_k \langle \psi(\theta) | P_k | \psi(\theta) \rangle$. The exact values of the a_k coefficients as well as the specific choice of Pauli gates, depend on the employed fermionic to qubit operator mapping, e.g. Jordan-Wigner (JW) [20], Bravi-Kitaev [58] and more (see [9] and references therein), here we refer to the standard JW mapping.

3 The VQ-SCI Method

The proposed quantum variational SCI (VQ-SCI) algorithm is depicted in Alg. 1. It deviates from classical SCI algorithms in that the second phase of finding the groundstate of the SCI matrix M_{CI} is performed via quantum computing; In what follows we describe each step of the quantum part in more details and provide a step-by-step description for the case of the H_2 molecule.

Algorithm 1 Variational Quantum SCI (VQ-SCI) algorithm

1. Construct the SCI matrix (classical):
 - (a) Select a set of Slater determinants using any favorable SCI algorithm.
 - (b) Order the Slater determinants.
 - (c) Construct the M_{CI} matrix in the form of Eq. 5.
 2. Find the groundstate of the SCI matrix (quantum):
 - (a) Map the Slater determinants to computational basis states.
 - (b) Encode the Hamiltonian matrix to a qubit operator.
 - (c) Find the M_{CI} groundstate via a variational quantum circuit.
-

3.1 Finding the groundstate of the SCI matrix

Mapping the Slater determinants to computational basis states

Given the ordered set of Slater determinants, we map the k^{th} determinant to the k^{th} computational basis state $\chi_{k \rightarrow} |k\rangle = |b_0^k b_1^k \dots b_{q-1}^k\rangle$, $b_j^k \in \{0, 1\}$, using standard binary encoding $k = \sum_{j=0}^{q-1} 2^j b_j^k$ (any other decimal-to-binary encoding will also do). This requires $q = \lceil \log_2(D) \rceil$ qubits to encode D Slater determinants.

Hamiltonian encoding in the computational basis

Using the computational basis states $|k\rangle$ the M_{CI} matrix can be encoded as:

$$M_{CI} = \sum_{j,k=0}^{D-1} M_{CI}(j,k) |j\rangle\langle k|, \quad (9)$$

with $M_{CI}(j,k) = \langle j|M_{CI}|k\rangle = \langle \chi_j | M_{CI} | \chi_k \rangle$, corresponding to Eq. 5. Next note that each matrix index $|j\rangle\langle k|$ can be encoded to a qubit operator using a tensor product of q single-qubit operators as follows (see e.g. [37]):

$$|j\rangle\langle k| = \bigotimes_{n=0}^{q-1} |b_n^j\rangle\langle b_n^k| \quad (10)$$

where each single qubit operator $|b_n^j\rangle\langle b_n^k|$ is given by one of the following four possible single-qubit operators:

$$\begin{aligned} |0\rangle\langle 0| &= \frac{1}{2}(I + Z), & |0\rangle\langle 1| &= \frac{1}{2}(X + iY) \\ |1\rangle\langle 0| &= \frac{1}{2}(X - iY), & |1\rangle\langle 1| &= \frac{1}{2}(I - Z) \end{aligned} \quad (11)$$

which can be expressed as a simple sum of two Pauli gates:

$$|b_n^j\rangle\langle b_n^k| = \frac{1}{2}(\sigma_a + i^p \sigma_b)_{jk}, \quad \sigma_a \in \{I, X\}, \sigma_b \in \{Z, Y\} \quad (12)$$

Overall, the resulting qubit operator is given by:

$$M_{CI} = \sum_{k,j=0}^{D-1} M_{CI}(j, k) \bigotimes_{n=0}^{q-1} |b_n^j\rangle\langle b_n^k| = \sum_{k,j=0}^{D-1} M_{CI}(j, k) \bigotimes_{n=0}^{q-1} \frac{1}{2} \left(\sigma_a^{(n)} + i^p \sigma_b^{(n)} \right)_{jk} \quad (13)$$

which leads, after multiplying the q parentheses to:

$$\frac{1}{2^q} \sum_{j,k=0}^{D-1} M_{CI}(j, k) \sum_{l=1}^{2^q} i^{\vec{p}} \bigotimes_{n=0}^{q-1} \sigma_l^{(n)} \quad (14)$$

where $i^{\vec{p}} \in \{\pm 1, \pm i\}$, and $\sigma_l^{(n)} \in \{I, X, Y, Z\}$ is a Pauli operator applied to the n^{th} qubit, so that each matrix index is encoded by $2^q = D$ Pauli strings of length q .

Note that the matrix entries, $M_{CI}(j, k)$, themselves are not encoded to the quantum circuit. Instead, they are calculated classically through Eq. 5 and either stored simply as a D by D matrix or calculated on demand. Further, the encoding of the Hamiltonian operator to the quantum circuit is different from that employed in VQE, as it encodes matrix indices rather than fermionic operators. It is also different than the encoding in [39], in which each excitation operator is separately encoded to the circuit. This introduces constraints to the choice of configurations, which resulted with a larger number of qubits.

Finally, given the SCI Hamiltonian matrix encoded in the computational basis, we find its groundstate by optimizing a parameterized quantum circuit in the known variational manner of Eq. 6.

3.1.1 The H_2 molecule - a detailed example with a single qubit

Below is a step-by-step description of the groundstate energy calculation for the H_2 molecule using a single qubit via VQ-SCI, as outlined in Alg. 1.

Step I - Selecting the Slater determinants

The H_2 molecule ($N=2$ electrons) has $M=4$ spin-orbitals in the sto-3g basis set, which result with $D_{FCI} = \binom{2}{1} \binom{2}{1} = 4$ possible spin-restricted configurations:

$$\begin{aligned} \Phi_0 &= SD\{\sigma_{1s,g\downarrow}, \sigma_{1s,g\uparrow}\}, & \Phi_2 &= SD\{\sigma_{1s,u\downarrow}, \sigma_{1s,g\uparrow}\} \\ \Phi_1 &= SD\{\sigma_{1s,u\downarrow}, \sigma_{1s,u\uparrow}\}, & \Phi_3 &= SD\{\sigma_{1s,g\downarrow}, \sigma_{1s,u\uparrow}\} \end{aligned} \quad (15)$$

where each spin-orbital takes the *gerade* or the *ungerade* spatial symmetry.

In this simple case we can select the most dominant Slater determinants using solely symmetry considerations (in all other cases we use a different scheme, see Sec. 4.2): the exact groundstate of H_2 is known to be of the *gerade* symmetry, and hence cannot consist of Slater determinants that do not obey this symmetry. In particular, single excitation determinants with *ungerade* symmetry must be excluded [2]. This leaves us with only two allowed Slater

determinant: Φ_0 and Φ_1 , where Φ_0 is the single-determinant HF solution and Φ_1 is the double excitation state relative to it. In this case the SCI groundstate is hence identical with the FCI groundstate.

Step II - Ordering the Slater determinants

In this step each Slater determinant is mapped to a particular computational state. Here, we perform the direct mapping:

$$\Phi_0 \rightarrow |0\rangle, \quad \Phi_1 \rightarrow |1\rangle, \quad (16)$$

with which the H_2 groundstate is given by

$$\psi = c_0\Phi_0 + c_1\Phi_1 = c_0|0\rangle + c_1|1\rangle, \quad |c_0|^2 + |c_1|^2 = 1. \quad (17)$$

In principle, we could employ the opposite mapping, but the direct mapping of Eq. 16 is better because it is less prone to measurement errors. It maps the HF solution of Φ_0 , which constitutes a significant portion of the final state (this is also the case for other molecules), to the $|0\rangle$ state. An error in measuring the $|0\rangle$ state is often less probable than in measuring the $|1\rangle$ state.

Step III - Constructing the 2-dimensional SCI matrix

Constructing the 2-dimensional SCI matrix M_{CI} , is performed by classical methods. Here, we used psi4 [59] to calculate it, as follows:

$$M_{CI} = \begin{bmatrix} \langle \Phi_0 | \mathcal{H} | \Phi_0 \rangle & \langle \Phi_0 | \mathcal{H} | \Phi_1 \rangle \\ \langle \Phi_1 | \mathcal{H} | \Phi_0 \rangle & \langle \Phi_1 | \mathcal{H} | \Phi_1 \rangle \end{bmatrix} = \begin{bmatrix} -1.8266 & 0.1814 \\ 0.1814 & -0.2596 \end{bmatrix} = \begin{bmatrix} \langle 0 | \mathcal{H} | 0 \rangle & \langle 0 | \mathcal{H} | 1 \rangle \\ \langle 1 | \mathcal{H} | 0 \rangle & \langle 1 | \mathcal{H} | 1 \rangle \end{bmatrix} \quad (18)$$

where \mathcal{H} is the Hamiltonian of the H_2 molecule, evaluated at the equilibrium bond length of 0.745 Ang and the last equality term stems from the mapping in Eq. 16 (see a similar calculation in [60] for 1.4 [au] = 0.7408 Ang bond length).

Step IV - Encoding the SCI matrix to Pauli operators

Given the SCI matrix M_{CI} in the computational basis, it is next translated to a linear combination of Pauli operators, using the decomposition of Eq. 11:

$$\begin{aligned} M_{CI} &= -1.8266|0\rangle\langle 0| + 0.1814|0\rangle\langle 1| + 0.1814|1\rangle\langle 0| - 0.2596|1\rangle\langle 1| \quad (19) \\ &= -1.0431\hat{I} - 0.7835\hat{Z} + 0.1814\hat{X} \end{aligned}$$

While this step is conceptually simple, it adds a large classical computational overhead, see Sec. 5.

Step V - Finding the groundstate of the SCI matrix

Once the H_2 SCI matrix is decomposed to Pauli operators, we find its lowest eigenvalue via the standard variational quantum scheme. Since we only use a

single qubit and since the SCI matrix and hence the groundstate are both real, our Ansatz circuit consists only of a single qubit R_y rotation:

$$\psi(\theta) = R_y(\theta)|0\rangle = \cos\left(\frac{\theta}{2}\right)|0\rangle + \sin\left(\frac{\theta}{2}\right)|1\rangle. \quad (20)$$

For comparison, in the standard VQE with JW encoding the H_2 groundstate in the sto-3g basis set is represented as $\psi(\theta) = \cos(\frac{\theta}{2})|1100\rangle + \sin(\frac{\theta}{2})|0011\rangle$ using 4 qubits, and 2 qubits are required when the parity encoding is employed [12].

4 Results

4.1 Computational setup and hyper-parameters

We ran the proposed VQ-SCI method for the following set of molecules: H_2 , LiH, BeH_2 , H_2O , NH_3 , and C_2H_4 in the sto-3g basis set, under spin-restriction form, as defined above, see Figs. 3-4 and Table 1 for a concise summary.

We computed the groundstate of each molecule using: (a) the full-CI (FCI) groundstate energy, calculated classically via diagonalization of the FCI matrix, using the psi4 chemistry package [59] (dashed green line); (b) selected CI groundstate energy, calculated classically via diagonalization of the SCI matrix, using standard numerical Python diagonalization (gray diamonds); (c) noiseless statevector classical simulations of the VQ-SCI scheme (blue circles); (d) noisy classical simulations of the VQ-SCI scheme (purple triangles) through the "ibmq_qasm" simulator platform using 100k shots (maximum allowed, except for H_2 and LiH, where we used 20k shots), where in order to have a common frame of reference we used the noise model of "ibmq_santiago" (except for H_2 molecule where we used "ibmq_lima"); and (e) real IBMQ hardware calculations (red squares) using 20k shots (maximum available). The specific hardware selection depended mainly on number of qubits and availability. In the noisy and real-hardware executions we used a standard measurement error mitigation, based on a calibration matrix [61], as implemented by Qiskit. For calculations on real devices, the entire variational procedure was performed, rather than starting from optimal parameters found on a noisy simulator, as done sometimes in the literature.

SCI matrices are hermitian by definition. Here the SCI matrices are further real (symmetric) with real eigenvectors, since they are constructed in a basis of real Slater determinants (in the sto-3g basis set). This entails that the variational search can be confined to unitary transformations on the real plain. We therefore used Qiskit RealAmplitudesAnsatz (with circular entanglement), see Fig. 2, which is only composed from single qubit R_y -rotations and CNOT gates, both preserve real amplitudes of the quantum state. For each system, we set the number of circuit layers to be the minimal one with which chemical accuracy was reached using noiseless simulations. We didn't optimize over the choice of the circuit Ansatz. We used the COBYLA optimizer [62] throughout as implemented within Qiskit [63]. We didn't optimize over that choice either.

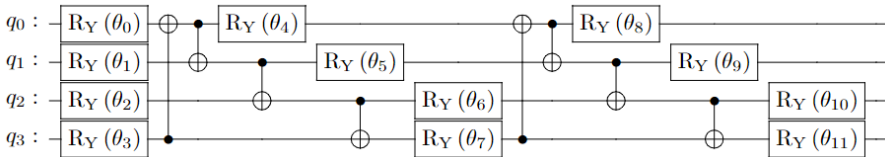


Fig. 2: The RealAmplitude circuit Ansatz, illustrated for the case of $q = 4$ qubits and $L = 2$ entangling layers. The zero'th layer consists of only R_Y rotations, where each further layer has $q = 4$ CNOT gates and one R_Y rotation, per qubit.

The average and standard deviation of the groundstate energy were computed for noiseless simulation, noisy simulation and real hardware using the last 10 VQE iterations results, except for the H_2O molecule where we ran each VQE noisy simulation 10 times and averaged the resulting energies of the last iteration, to reach more reliable results.

In all calculations the initial state was the HF state. The optimizer convergence was usually achieved within 50 iterations, except for the H_2O molecule where the real hardware computation took almost 100 iterations.

The Slater determinants were obtained by running a restricted Hartree-Fock computation, resulting with a set of molecular orbitals, and then constructing all possible spin-restricted Slater determinants from the set of molecular orbitals (the method, however, is not constrained to the spin-restricted form). The FCI groundstate wavefunction can be computed classically by common software packages. For this work we used the psi4 chemistry package to perform all of the above classical computations [59]. Next we describe how we chose the D_{SCI} most significant Slater determinants.

4.2 Choosing the most significant Slater determinants

Selecting D dominant Slater determinants can be done by various classical SCI schemes, each comes with its own efficiency and accuracy [40, 42, 51, 64]. Here, however, we were not interested in the details of the selection method and therefore took a simpler route. We performed a classical FCI calculation and ranked the configurations by their weight (absolute value of their amplitude) in the superposition groundstate.

Next, we chose the $D_{SCI} = 2^q$ most dominant (largest weight) Slater determinants by searching for the minimal q which resulted with groundstate energy that reached chemical accuracy with respect to the FCI energy. In practice, we simply doubled the number of configurations, corresponding to increasing the number of qubits by 1, until chemical accuracy was achieved. This is the method we used to generate the VQ-SCI curve in Fig. 1. For practical calculations, when the FCI energy is not known in advance, one can increase the number of configuration until a predefined accuracy threshold is reached.

We employed a simple decimal-to-binary mapping between Slater determinants and the computational basis following the Slater determinants significance order (with $\phi_0 = \phi_{HF}$ being the most significant Slater determinant and ϕ_{2^q-1} being the least significant): $\phi_0 \rightarrow |0\rangle^{\otimes q}, \dots, \phi_{2^q-1} \rightarrow |1\rangle^{\otimes q}$. As

already mentioned in Sec. 3.1.1, the advantage in mapping $\phi_0 = \phi_{HF} \rightarrow |0\rangle^{\otimes q}$ is that it lessens the effect of measurement errors, as the weight of the HF state in the final groundstate is relatively high. For the same reason we also initialize the variational quantum state to $|0\rangle^{\otimes q}$.

4.3 Small molecules: H₂, LiH, and BeH₂

The top row of Fig. 3 presents potential energy curves (groundstate energy as a function of interatomic distance) of the H₂, LiH, and BeH₂ molecules, as obtained with VQ-SCI, in comparison to the exact FCI results. To get a closer look at the method’s accuracy, the bottom row of Fig. 3 shows the deviation from the exact FCI results, as a function of interatomic distance, where the green area marks the chemical accuracy regime (0.0016 Ha) around the FCI result, the gray area marks the chemical accuracy regime around the SCI results, and the error bars indicate standard deviation.

The H₂ molecule - one qubit

Calculating the groundstate of the H₂ molecule (2 electrons, 4 spin-orbitals) with VQ-SCI requires a single qubit, as described in Sec. 3.1.1. This enables the usage of the shallowest possible quantum circuit, with a single Ry rotation gate and no controllers. It is seen in the H₂ potential energy curve of Fig. 3a that the VQ-SCI energies follow closely the exact FCI curve even when executed on real device (“ibmq_lima”). The higher resolution of the error curve in Fig. 3d further reveals that the noiseless statevector simulation practically coincides with the exact FCI results, and that both the noisy simulation and the real-hardware results reach chemical accuracy, up to standard deviation, throughout. In particular, for the near equilibrium bond length of 0.7 Ang, the real-hardware groundstate energy is $\Delta E = |E - E_{FCI}| = 0.001$ Ha from the FCI solution, well within the chemical accuracy region.

To facilitate a clear comparison of the obtained accuracy with those reported in the literature, Table 1 summarizes (to the best of our knowledge) previous real-hardware groundstate calculations of the molecules studied in this work, at the equilibrium geometry, alongside with our real-hardware results. The Table reveals that reaching chemical accuracy via VQE (or alike) on recent and current quantum devices is still not a trivial task, even for the small H₂ molecule in the minimal sto-3g basis set (in contrast, phase-estimation based schemes reached very high accuracy for H₂, much beyond chemical accuracy [60, 65], but are not scalable). For example, real-hardware VQE calculations of the H₂ molecule reported in [12] used two qubits and reached energy that is roughly 0.02 Ha away from the exact FCI solution. A better accuracy of 0.01 Ha was obtained in [14] using a single layered circuit. In the work of [39] the H₂ molecule was computed on real quantum devices for the larger 6-31 basis set using 4 qubits, reaching an energy deviation of roughly 0.01 Ha from the corresponding FCI solution. In the work of [66] the H₂ groundstate was computed through the variational quantum computed moments (QCM) method (introduced in [67]) using 2 qubits. The obtained groundstate energy

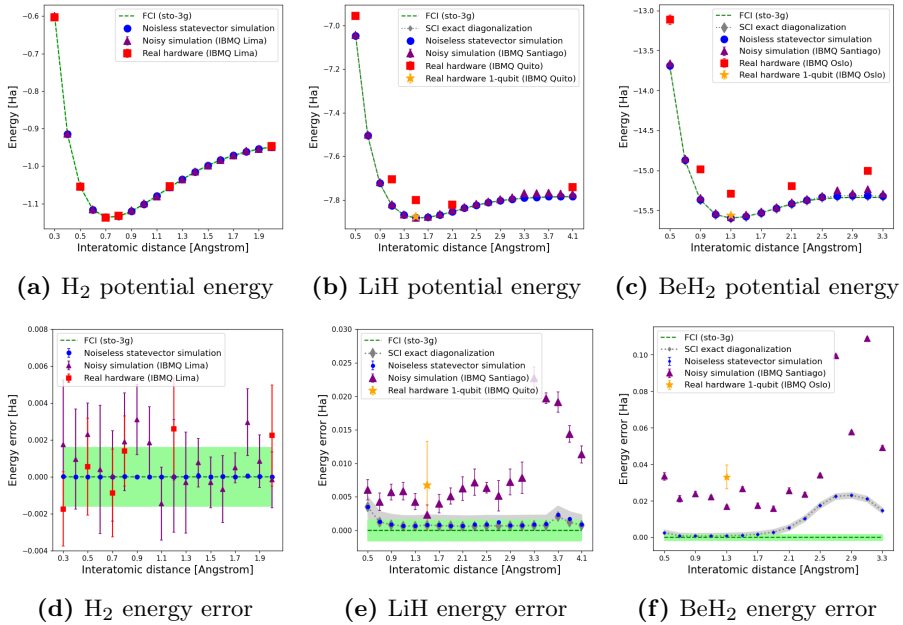


Fig. 3: Top row: the VQ-SCI groundstate energy [Ha] as function of the interatomic distance [Ang], for H₂ (1 qubit), LiH (3 qubits), and BeH₂ (4 qubits). The dashed green represents the full-CI (FCI) groundstate energy, calculated classically via diagonalization of the SCI matrix; Blue circles represent the SCI groundstate energy obtained by noiseless statevector classical simulations of the VQ-SCI scheme; Purple triangles indicate classical noisy simulations of the VQ-SCI scheme through the “*ibmqasm*” simulator; Red squares represent real IBMQ hardware VQ-SCI calculations using 20k shots (maximum available); Finally, the yellow stars in LiH and BeH₂ stand for VQ-SCI calculation on real IBMQ hardware, using just a single qubit which accounts for the two most significant Slater determinants. The error bars represent the standard deviation values, observed better in the scale of the bottom row. **Bottom row:** zoom-in to the energy error [Ha] with respect to the exact FCI values, depicted using the same color scheme as above. The green area represents the chemical accuracy region (0.0016 Ha) around the exact FCI energy, whereas the gray area represents the chemical accuracy region around the exact SCI energy. For comparison, the corresponding HF groundstate energies for the H₂, LiH, and BeH₂ molecules at the equilibrium geometry are -1.1173 Ha, -7.8633 Ha, and -15.5612 Ha, respectively; the exact FCI groundstate energies for H₂, LiH, and BeH₂ at the equilibrium geometry are -1.13618 Ha, -7.8823 Ha, and -15.59504 Ha, respectively.

deviated by $\Delta E = 0.001$ Ha from the FCI solution, thereby reaching chemical accuracy. Finally, a recent study reached chemical accuracy with standard VQE for the H₂ molecule via a direct pulse engineering approach, using 2 qubits [68]. Reaching chemical accuracy was enabled in our H₂ calculations, despite being executed on the standard gate-based model, due to our minimal single-qubit circuit, which introduced relatively low noise.

The LiH molecule - 3 qubits

The LiH molecule (4 electrons, 12 spin-orbitals) requires 8 Slater determinants to reach chemical accuracy within the sto-3g basis set, encoded with 3 qubits. Two circuit layers were required for reaching chemical accuracy on noiseless

VQ-SCI simulations, and were thus employed also in the real-hardware calculations. Fig. 3b shows the potential energy curve of LiH as calculated by the VQ-SCI. It is seen that the noiseless and noisy calculations closely resemble the FCI curve, but that the real hardware results (“ibmq-quito”), deviate by ~ 0.1 Ha (with $\Delta E = 0.081$ Ha at the equilibrium bond length of 1.5 Ang).

Fig. 3e presents the corresponding error energy curve. It is seen that the exact SCI results are slightly higher than the exact FCI results, but are well within the FCI chemical accuracy (except for the 3.7 Ang interatomic distance). The noiseless results are almost identical with the exact SCI diagonalization, and the noisy simulation results deviate by few mili-Hartrees from the exact SCI curve. The real-hardware results (red square) are not included in Fig. 3e to maintain high resolution. It is also seen that the error (both noiseless and noisy results) increases with bond length. This is observed also in the standard VQE scheme and reflects the difficulty in accurately describing highly correlated systems, see e.g. [69].

For comparison with previous real-hardware groundstate calculations of LiH in the sto-3g basis set, see Table 1. We note that: first, in [14] 4 qubits were used, after freezing two spin-orbitals. The classical simulation required 6 layers, assuming an all-to-all qubit topology; Best experimental result was achieved with zero layers and reached energy of $\Delta E = \sim 0.05$ Ha away from the exact FCI energy, at the 1.5 Ang equilibrium bond-length, see Fig. S9(b) in [14]; second, in [17] LiH was calculated with VQE using 4 qubits (the two core electrons were frozen) through symmetry preserving circuits (SPC), reaching approximately $\Delta E = 0.0025$ Ha. The scheme of quantum imaginary time evolution (QITE) was also employed in [17] using 2 qubits (following core electrons freezing and reduced Hamiltonian blocks), reaching groundstate energy with approximately $\Delta E = 0.005$ Ha; and finally, the recent work of [39] on LiH (at an interatomic distance of 1.55 Ang) used 4 qubits and reached an error of approximately $\Delta E \approx 0.01$ Ha. Both [17] and [39] utilized the Richardson extrapolation method for noise mitigation, which we so far did not use.

We further calculated the groundstate energy at the equilibrium bond length using only the two most significant Slater determinants. This required a single qubit and a single Ry rotation gate (as in H_2). The real-hardware result, marked by a yellow star, is shown in Figs. 3b and 3e. Such a calculation illustrates a trade-off between *accuracy*, achieved by increasing the number of Slater determinants, and *precision*, which deteriorates with increasing the number of qubits, due to the presence of more noise. In the case of LiH, SCI with two Slater determinants deviates from the exact FCI energy by ~ 0.0055 Ha. A similar accuracy was reproduced with real-hardware calculation. This is because of the high precision of the real-hardware single qubit calculation, as we saw before with H_2 . Figs. 3b and 3e indicate that in the case of LiH, the shortage of Slater determinants is largely compensated by a significant noise reduction, reaching $\Delta E = 0.007$ Ha from the FCI result.

The BeH₂ molecule - 4 qubits

The BeH₂ molecule (6 electrons, 14 spin-orbitals) requires 16 Slater determinants to reach chemical accuracy with respect to the FCI groundstate energy, which we encode using 4 qubits. The VQ-SCI required 3 layers to reach chemical accuracy on noiseless simulation. Using the same number of layers, real-hardware calculation at the equilibrium bond length of 1.3 Ang, reached an error of approximately 0.3 Ha, see Fig. 3c. Fig. 3f demonstrates that as the atoms separate the SCI with 16 Slater determinants is no longer sufficient, as the SCI energy is no longer within the chemical accuracy region.

In comparison with previous literature, 6 qubits were used in [14] after ignoring the $2p_y, 2p_z$ orbitals per spin-channel (total of 4 spin-orbitals), freezing 2 spin-orbitals, and tapering off 2 qubits. Noiseless simulation required 16 layers assuming an all-to-all qubit topology. Best experimental result, at the equilibrium bond-length, was achieved with zero layers and reached groundstate energy which deviated by more than $\Delta E = 0.25$ Ha from the exact FCI energy, see Fig. 3 in [14].

As in the case of LiH, we further performed a single-qubit, real-hardware, VQ-SCI calculation of BeH₂ groundstate at the equilibrium bond length, accounting for only 2 Slater determinants. This calculation reached a relatively high accuracy of $\Delta \approx 0.035$ Ha, as marked by the yellow star in Figs. 3c and 3f.

4.4 Larger molecules: water, ammonia, and ethylene

Fig. 4 shows the VQ-SCI results for the H₂O, NH₃, and C₂H₄ molecules. For each molecule the convergence of the groundstate energy is shown as a function of the number of significant Slater determinants, selected as described in Sec. 4.2. All calculations were performed at a fixed molecular geometry, as detailed per molecule.

The H₂O molecule (water) - 5 qubits

The ground-state energy of the H₂O molecule (10 electrons, 14 spin-orbitals) was calculated at a fixed equilibrium geometry of O-H bond-length 0.955 [Ang] and an angle of 105°, as in [16]. Applying spin-restriction to the wavefunction results with a total of 441 possible Slater determinants. Yet, as entailed by Fig. 4a, 32 determinants are already sufficient for reaching the chemical accuracy (green area), thereby requiring merely 5 qubits. We used {0, 1, 2, 3, 5} layers for 1 – 5 qubits, respectively, except for the noisy simulation of 5 qubits for which we used only 4 layers. For the noisy simulation we used up to 300 iterations and 100k shots, whereas using real-hardware we used up to 100 iterations and 20k shots (due to real-hardware availability). For each number of configurations, the noisy simulation was performed 10 times to obtain more stable results, upon which we averaged and took the standard deviation.

We calculated the groundstate energy of the water molecule in the exact same basis and geometry as done in [16], which thus form a good reference point to our results. The VQE calculations reported in [16] employed the unitary coupled cluster (UCC) Ansatz, with a growing number of selected excitations.

Their classical simulations required 18 Slater determinants to reach chemical accuracy, which were encoded with 11 qubits and 143 entangling gates. In comparison, our VQ-SCI simulations recovered the FCI energy to chemical accuracy with 5 qubits and 25 CNOT gates, demonstrating the practical significance of the method.

A similar trend is observed in the real-hardware calculations. The real hardware calculations reported in [16] were performed on an ion-trap quantum computer. They accounted for 2 (HF+1) and 4 (HF+3) Slater determinants using 2 and 3 qubits, and employed 2 and 6 XX gates, respectively, reaching precision deviations of up to 0.004 Ha from the exact SCI diagonalization curve. Our real-hardware calculations for 2 and 4 Slater determinants on IBM machines used 1 and 2 qubits, and employed zero and one CNOT gate (before transpiling), respectively. These calculation reached precision deviations of at most 0.003 Ha from the exact SCI diagonalization curve, see Fig. 4a.

The VQ-SCI results are shown to be more precise than those reported in [16]. This is despite the fact that the superconducting qubit technology we used is more susceptible to decoherence noise than the ion-trap quantum technology and that several hardware optimizations were carried in [16] in a co-design framework, with no external limitations on the number of shots. The central reason for this relative success is the use of a shallower circuit Ansatz with fewer qubits, enabled by our encoding.

We further note that the water molecule was also calculated previously using 5 qubits in [29] on real IBM hardware, to very good accuracy. This was done by using core-freezing, accounting for only 6 electrons in 10 spin-orbitals, and by employing the entanglement forging method.

The NH_3 molecule (ammonia) - 6 qubits

We calculated the groundstate energy of the Ammonia molecule NH_3 (10 electrons, 16 spin-orbitals) at the HF (sto-3g) equilibrium geometry with N-H distance of 1.0325 Ang and H-H distance of 1.6291 Ang, as taken from [70]. Fig. 4(b) shows that chemical accuracy can be reached with 64 Slater determinants using 6 qubits, in contrast to 16 qubits that would be required in the standard VQE. While our noisy simulations matched the noiseless simulation quite well up to 3 qubits, the real-hardware results deviated by almost 0.02 Ha already for two qubits.

The C_2H_4 molecule (ethylene) - 12 qubits

Ethylene (16 electron, 28 spin-orbitals) is the largest molecule we addressed. The geometry of the molecule was defined according to HF ground state energy in equilibrium geometry in the sto-3g basis, as given in [70] (see appendix A). Using the sto-3g minimal basis under spin-restricted form results with $\binom{14}{8}^2 = 9,018,009$ Slater determinants. Fig. 4(c) shows the groundstate energy of ethylene as a function of the number of selected Slater determinants. It is seen that 4096 Slater determinants are sufficient for obtaining chemical accuracy, which can be simulated with 12 qubits.

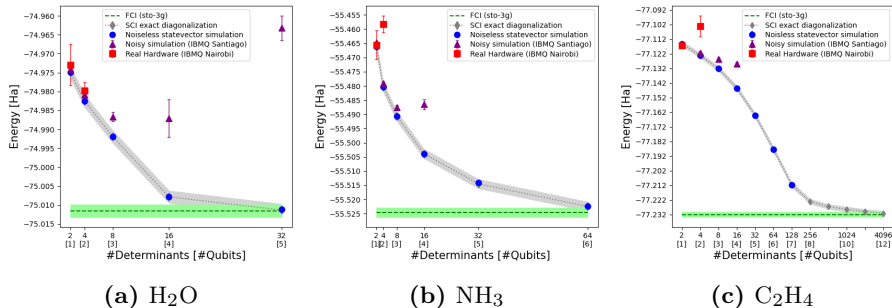


Fig. 4: The groundstate energy [Ha] as a function of the number of significant Slater determinant configurations, corresponding to a growing number of qubits, for the H₂O, NH₃, and C₂H₄ molecules, calculated at the equilibrium geometry. The dashed green line represents the full-CI (FCI) groundstate energy, where the green area marks the chemical accuracy region (0.0016 Ha); Gray diamonds with dotted line represent the SCI groundstate energy, calculated classically via diagonalization of the SCI matrix, where the gray area marks the chemical accuracy region around the exact SCI solution; Blue circles represent the SCI groundstate energy obtained by noiseless statevector classical simulations of the VQ-SCI scheme; Purple triangles indicate classical noisy simulations of the VQ-SCI scheme through the “*ibmq.qasm*” simulator; Red squares represent real IBMQ hardware VQ-SCI calculations using 20k shots (maximum available); The error bars represent the standard deviation values. For comparison, the corresponding HF groundstate energies for the H₂O, NH₃, and C₂H₄ molecules are -74.9624 Ha, -55.4554 Ha, and -77.07395 Ha, respectively; the exact FCI groundstate energies for H₂O, NH₃, and C₂H₄ are -75.01156 Ha, -55.52431 Ha, and -77.2321 Ha, respectively

Our noiseless simulation for $\{1, 2, 3, 4, 5, 6, 7\}$ qubits were performed with $\{0, 1, 2, 3, 7, 11, 18\}$ layers, respectively. We performed up to 500 iterations in all cases. Note that here we did not go beyond 7 qubits, due to the runtime consumption of our current implementation, which scales as D^3 , but can be significantly improved, see Sec. 5. We are not aware of previous real-hardware groundstate energy calculations of the ethylene molecule.

5 Resource analysis and discussion

As all variational quantum algorithms, the VQ-SCI algorithm requires quantum and classical resources. On the quantum side, it requires $\log D$ qubits and $O(LP SI)$ circuit executions, where L is the number of layers in the quantum circuit, P is the number of distinct Pauli-strings that have to be measured, S is the number of shots required to achieve a certain statistical accuracy per Pauli string measurement, and I is the number of required iterations. On the classical side, the VQ-SCI requires computing and storing D Slater determinants, the computation of P Pauli strings and the optimization of $O(L \log D)$ variational parameters (one parameter per qubit times L layers), per iteration.

In terms of the required number of qubits, the VQ-SCI method offers a significant advantage in comparison to standard VQE, as shown in Fig. 1 and discussed in Sec. 1.1. Yet, in terms of execution time, the VQ-SCI scales quadratically with D_{SCI} , which, for large molecules, can be intractable. To see that, we focus on P , the number of Pauli strings, which accounts for most

Mol.	Ref. (year)	#Qubits	Δ FCI (Ha)	QC	Remark
H ₂	[65] (2010)	2	10 ⁻⁶	Photonic	IPEA*
	[60] (2010)	2	10 ⁻¹³	NMR	PEA*
	[12] (2016)	2	0.02	Xmon	PEA*
	[12] (2016)	2	0.02	Xmon	
	[14] (2017)	2	0.01	IBM	
	[39] (2022)	4	0.01	IBM	6-31G basis set
	[66] (2022)	2	0.001	IBM	QCM*
	[68] (2022)	2	0.001	IBM	Pulse engineering
This work	1	0.001	IBM		
LiH	[14] (2017)	4	0.05	IBM	
	[17] (2021)	4	0.0025	IBM	COF + EE
	[17] (2021)	2	0.005	IBM	QITE* + COF + EE
	[39] (2022)	4	-0.01	IBM	EE
	This work	3	0.081	IBM	
This work*	1	0.007	IBM		
BeH ₂	[14] (2017)	6	0.25	IBM	
	This work	4	0.3	IBM	
	This work*	1	0.035	IBM	
H ₂ O	[16] (2020)	(11) 3	0.028	IonQ	(18) 4 SDs
	[29] (2022)	5	0.007	IBM	COF
	This work*	(5) 2	0.032	IBM	(32) 4 SDs
NH ₃	This work*	(6) 1	0.06	IBM	
C ₂ H ₄	This work*	(12) 1	0.12	IBM	

Table 1: A summary of groundstate calculations of the molecules studied in this paper, in equilibrium geometry, performed on real quantum hardware, as reported in the literature, and ordered chronologically. For each study we specify the number of qubits used in the experiment (numbers in parentheses indicate how many qubits are required to reach the FCI solution), the deviation from the FCI solution in Hartree, and the quantum hardware technology that was used. The calculations were done in the sto-3g basis set, unless otherwise stated. It is evident that the VQ-SCI consistently employs the least number of qubits, except for cases where core orbital freezing (COF) is used, which effectively accounts for a smaller number of electrons. All results from literature were obtained with VQE, unless marked with a star in the remark column. The following acronyms are used: phase estimation algorithm (PEA), iterative PEA (IPEA), quantum computed moments (QCM), error extrapolation (EE), quantum imaginary-time evolution (QITE), and Slater-determinants (SDs).

of the computational burden. Given D Slater determinants there are $4^q = D^2$ different Pauli strings of length q , which gives an upper bound for P . In the case of FCI, we have $D_{FCI}^2 = \binom{M/2}{N/2}^4$ different Pauli strings (assuming spin-restriction), which, in the worst case of $M = 2N$, scales exponentially with the number of spin-orbitals M . In contrast, in VQE the number of distinct Pauli strings scales polynomially with M ($\mathcal{O}(M^4)$). In the case of SCI, the relation between D_{SCI} and M and N depends on the particular selection method we use. Empirically we observe that in our case $D_{SCI} \approx \sqrt{D_{FCI}} = \binom{M/2}{N/2}$, which reduces the number of Pauli strings quadratically.

Fig. 5 shows the improvement of VQ-SCI over the VQ-FCI in terms of the required number of Pauli strings. Moreover, it demonstrates that for a large set of molecules the VQ-SCI requires the measurement of fewer Pauli strings than VQE. Yet, it still suffers from an intractable scaling. This can be partially remedied (so far we only considered an upper bound for P) by taking the

hermiticity of the Hamiltonian into account and by employing methods such as the tensor product basis (TPB) method [8, 14, 27, 71].

It is also instructive to consider the required number of Pauli strings for an increasing basis set, i.e. the case where the number of electrons (N) is kept fixed, while the number of spin-orbitals (M) increases. Using the estimated relation $D_{SCI} \approx \binom{M/2}{N/2}$ and relying on $\lim_{K \rightarrow \infty} \binom{K}{L} \approx \frac{K^L}{L!}$, we get that $D_{SCI} \approx \frac{(M/2)^{N/2}}{(N/2)!}$ and $P_{SCI} \approx \frac{(M/2)^N}{((N/2)!)^2}$. For small molecules or for calculations with small active space (small N), calculated in large basis sets (large M) this can be advantageous in comparison to VQE, as demonstrated in Appendix B. Note further that in this case the number of qubits required by VQ-SCI is exponentially smaller than that required by VQE (M), since $\log(D_{SCI}) \approx \frac{N}{2} \log \frac{M}{2}$, as also observed in [39].

The VQ-SCI offers great flexibility. It can directly choose any subset of Slater determinants, thereby reducing the number of required qubits, while still using relatively shallow circuits. The usage of shallower circuits effects both the induced noise as well as the number of overall circuit executions. This is because each variational parameter in the circuit Ansatz requires further circuit executions for the sake of the optimization process. Our resource analysis neglected the effect of the actual number of variational parameters in the quantum circuit. This number is relevant for the overall execution time and can be largely reduced by the reduction in the number of qubits, thereby reducing the actual runtime gap between VQE and VQ-SCI.

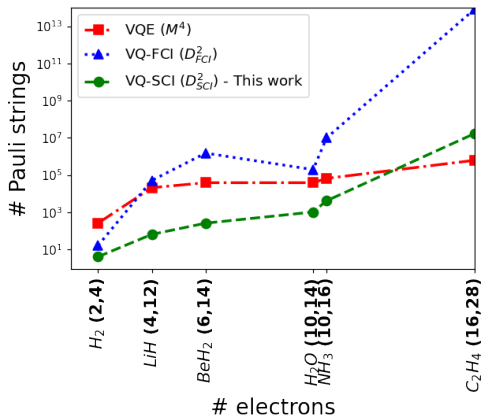


Fig. 5: The number of Pauli strings required to perform groundstate energy calculations of the molecules studied in this paper, ordered by their number of electrons (the NH_3 molecule is slightly shifted for clarity), in the sto-3g basis set, per method.

5.1 Mitigating the classical memory bottleneck

One of the most severe obstacles in classical SCI computation is the memory bottleneck [40, 51]. Most often an explicit storage of the SCI matrix is avoided by calculating it on the fly. Similarly, keeping an explicit list of the Slater determinants can be avoided, especially when the selection is done *a-priori*, by a fixed rule, such as in CISD, see [72] and references therein. The central memory (and time) bottleneck originates in finding the groundstate of the D -dimensional M_{SCI} matrix, where $D = D_{SCI}$. Classical SCI schemes employ iterative schemes such as the Davidson algorithm which finds the groundstate of a given D -dimensional matrix in $\mathcal{O}(D^2)$ time and $\mathcal{O}(D)$ memory [57]. As D can reach the order of 10^{12} determinants, see e.g. [73], the classical computation is often parallelized between many cores, which has a high communication cost.

The VQ-SCI offers a bypass to this classical memory bottleneck. This can be done by computing non-zero matrix elements sequentially and generating the Pauli strings one by one, per matrix entry, on the fly. This will exponentially reduce the classical storage requirement to $\log D$ for holding only the $\log D$ 2-qubit gates that encode the relevant matrix index-operator, see Eq. 10. Importantly, this exponential improvement in memory consumption can only be achieved when running the VQ-SCI on real devices. Simulating it classically will not benefit from calculating the Pauli strings on the fly. It would still require $2^q = D$ time and memory just to simulate the q -qubits circuit.

Reducing the classical memory comes at a computational time cost, as some Pauli strings will be measured multiple times. However, this approach is particularly suitable for the SCI matrix, which is very sparse. According to the Slater–Condon rules the matrix entries $M_{SCI}(j, k)$ (see Eq. 5) vanish whenever the Slater determinants Φ_j and Φ_k differ by more than two spin-orbitals [2]. This implies that each row has merely $\binom{N}{1}\binom{M-N}{1} + \binom{N}{2}\binom{M-N}{2} < N^2(M-N)^2 \ll D$ non-zero elements (in the spin un-restrictive case), where the exact sparsity will be dictated by the specific determinants selection (which may be initially done so as to increase sparsity). In conclusion, for a sparse D -dimensional matrix with $\mathcal{O}(D)$ non-zero entries (sparsity) and D Pauli strings per entry, the VQ-SCI method requires $\mathcal{O}(D^2)$ computational time (similar to the Davidson algorithm), but with $\log(D)$ memory (compared to $\mathcal{O}(D)$ in the case of Davidson algorithm).

6 Conclusion and outlook

We developed a framework for performing selected configuration interaction calculation through a variational quantum algorithm approach, denoted VQ-SCI. With this method we were able to simulate ground state calculations to FCI chemical accuracy for a set of small to medium size molecules, with the smallest to date number of qubits. The method uses a hardware efficient approach, while preserving the number of particles, and was shown to reach relatively high accuracy on IBM quantum devices, even without using advanced error mitigation schemes. Specifically, we reached chemical accuracy for the

H_2 molecule through a single qubit calculation, and performed real-hardware groundstate calculations of ethylene for the first time, using a small selected subset of significant Slater determinants.

The number of distinct Pauli strings that need to be measured in VQ-SCI scales worse than in VQE but can potentially outperform VQE for small-to-medium size molecules. Moreover, even for SCI of larger molecules, the overall number of circuit executions may eventually be larger in VQE due to the larger number of variational parameters it requires, in practice. For molecules for which the number of circuit executions is larger than in VQE, it may nevertheless be more feasible, simply due to its better noise resistance. The VQ-SCI may therefore be particularly valuable for the NISQ era, where qubits are scarce and noise is high. To reduce its time complexity, further research is required to minimize the number of needed measurements. To that end, it is worthwhile to: (a) explore the usage of Pauli grouping methods, such as TPB; (b) clarify the impact of other binary encodings, such as the Gray code, on the required resources; (c) find matrices which can be decomposed to small number of Pauli strings. For practical usage it is also beneficial to use more advanced error mitigation schemes.

In comparison to classical SCI methods, the VQ-SCI scales similarly in time, but offers an exponential reduction in memory consumption, which is a severe bottleneck in such classical computations. In that sense the VQ-SCI can potentially offer a practical advantage over classical eigensolvers, such as the Davidson algorithm.

Finally, the VQ-SCI provides a general quantum route for finding the groundstate of Hermitian matrices and can be used outside the chemical context, exhibiting the same advantage in memory scaling.

Acknowledgments. We acknowledge the use of IBM Quantum services for this work. The views expressed are those of the authors, and do not reflect the official policy or position of IBM or the IBM Quantum team.

Code availability. The underlying code for this study is available in GitHub and can be accessed via this link <https://github.com/danieli4444/SCI.VQE>.

Appendix A C_2H_4 geometry

For the C_2H_4 calculation we used the following HF equilibrium geometry, taken from NIST CCCBDB database [70]:

Appendix B Large basis sets

Fig. B2 shows the scaling of the required number of distinct Pauli strings when increasing the size of the basis set, namely when the number of electrons (N) is kept fixed, while the number of spin-orbitals (M) increases. It is seen that for small molecules in large basis sets, the VQ-SCI provides an advantage over VQE also in that respect. The yellow dotted line represent the estimation of

Atom	x (Å)	y (Å)	z (Å)
C1	0.000	0.000	0.653
C2	0.000	0.000	-0.653
H3	0.000	0.916	1.229
H4	0.000	-0.916	1.229
H5	0.000	-0.916	-1.229
H6	0.000	0.916	-1.229

Fig. A1: C_2H_4 equilibrium geometry corresponding to the HF solution.

$P_{SCI} = \frac{(M/2)^N}{(N/2)!^2}$ which is derived in the main text, based on the approximated relation $D_{SCI} = \sqrt{D_{FCI}}$. A very good fit is seen with the green curve, which estimates the number of Pauli strings with $P_{SCI} = D_{SCI}^2$, based on actual number of Slater determinants we used (D_{SCI}).

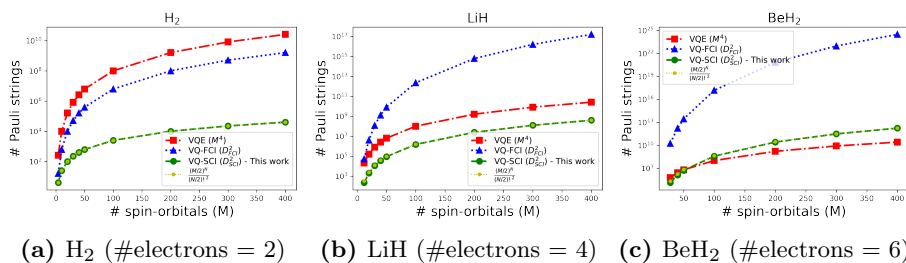


Fig. B2: The number of Pauli strings required per method, as a function of the number of spin-orbitals (M), for the H_2 , LiH , and BeH_2 molecules.

References

- [1] Dykstra, C., Frenking, G., Kim, K., Scuseria, G.: Theory and Applications of Computational Chemistry: the First Forty Years. Elsevier, [no place] (2011)
- [2] Szabo, A., Ostlund, N.S.: Modern Quantum Chemistry: Introduction to Advanced Electronic Structure Theory. Courier Corporation, [no place] (2012)
- [3] Hoffman, B.M., Lukoyanov, D., Yang, Z.-Y., Dean, D.R., Seefeldt, L.C.: Mechanism of nitrogen fixation by nitrogenase: the next stage. Chemical reviews **114**(8), 4041–4062 (2014)
- [4] Aspuru-Guzik, A., Lindh, R., Reiher, M.: The matter simulation (r) evolution. ACS central science **4**(2), 144–152 (2018)

- [5] Martin, R.M.: *Electronic Structure: Basic Theory and Practical Methods*. Cambridge university press, Cambridge (2020)
- [6] Saad, Y., Chelikowsky, J.R., Shontz, S.M.: Numerical methods for electronic structure calculations of materials. *SIAM review* **52**(1), 3–54 (2010)
- [7] Peruzzo, A., McClean, J., Shadbolt, P., Yung, M.-H., Zhou, X.-Q., Love, P.J., Aspuru-Guzik, A., O’Brien, J.L.: A variational eigenvalue solver on a photonic quantum processor. *Nature communications* **5**(1), 1–7 (2014)
- [8] McClean, J.R., Romero, J., Babbush, R., Aspuru-Guzik, A.: The theory of variational hybrid quantum-classical algorithms. *New Journal of Physics* **18**(2), 023023 (2016)
- [9] McArdle, S., Endo, S., Aspuru-Guzik, A., Benjamin, S.C., Yuan, X.: Quantum computational chemistry. *Reviews of Modern Physics* **92**(1), 015003 (2020)
- [10] Abrams, D.S., Lloyd, S.: Simulation of many-body fermi systems on a universal quantum computer. *Physical Review Letters* **79**(13), 2586 (1997)
- [11] Abrams, D.S., Lloyd, S.: Quantum algorithm providing exponential speed increase for finding eigenvalues and eigenvectors. *Physical Review Letters* **83**(24), 5162 (1999)
- [12] O’Malley, P.J., Babbush, R., Kivlichan, I.D., Romero, J., McClean, J.R., Barends, R., Kelly, J., Roushan, P., Tranter, A., Ding, N., *et al.*: Scalable quantum simulation of molecular energies. *Physical Review X* **6**(3), 031007 (2016)
- [13] Shen, Y., Zhang, X., Zhang, S., Zhang, J.-N., Yung, M.-H., Kim, K.: Quantum implementation of the unitary coupled cluster for simulating molecular electronic structure. *Physical Review A* **95**(2), 020501 (2017)
- [14] Kandala, A., Mezzacapo, A., Temme, K., Takita, M., Brink, M., Chow, J.M., Gambetta, J.M.: Hardware-efficient variational quantum eigensolver for small molecules and quantum magnets. *Nature* **549**(7671), 242–246 (2017)
- [15] Quantum, G.A., Collaborators*†, Arute, F., Arya, K., Babbush, R., Bacon, D., Bardin, J.C., Barends, R., Boixo, S., Broughton, M., Buckley, B.B., *et al.*: Hartree-fock on a superconducting qubit quantum computer. *Science* **369**(6507), 1084–1089 (2020)
- [16] Nam, Y., Chen, J.-S., Pimenti, N.C., Wright, K., Delaney, C., Maslov,

- D., Brown, K.R., Allen, S., Amini, J.M., Apisdorf, J., *et al.*: Ground-state energy estimation of the water molecule on a trapped-ion quantum computer. *npj Quantum Information* **6**(1), 1–6 (2020)
- [17] Yeter-Aydeniz, K., Gard, B.T., Jakowski, J., Majumder, S., Barron, G.S., Siopsis, G., Humble, T.S., Pooser, R.C.: Benchmarking quantum chemistry computations with variational, imaginary time evolution, and krylov space solver algorithms. *Advanced Quantum Technologies* **4**(7), 2100012 (2021)
- [18] Barison, S., Galli, D.E., Motta, M.: Quantum simulations of molecular systems with intrinsic atomic orbitals. *Physical Review A* **106**(2), 022404 (2022)
- [19] Kühn, M., Zanker, S., Deglmann, P., Marthaler, M., Weiß, H.: Accuracy and resource estimations for quantum chemistry on a near-term quantum computer. *Journal of chemical theory and computation* **15**(9), 4764–4780 (2019)
- [20] Jordan, P., Wigner, E.P.: über das paulische äquivalenzverbot. In: *The Collected Works of Eugene Paul Wigner*, pp. 109–129. Springer, [no place] (1993)
- [21] Cao, C., Hu, J., Zhang, W., Xu, X., Chen, D., Yu, F., Li, J., Hu, H., Lv, D., Yung, M.-H.: Towards a larger molecular simulation on the quantum computer: Up to 28 qubits systems accelerated by point group symmetry. *arXiv preprint arXiv:2109.02110* (2021)
- [22] Tilly, J., Chen, H., Cao, S., Picozzi, D., Setia, K., Li, Y., Grant, E., Wossnig, L., Rungger, I., Booth, G.H., *et al.*: The variational quantum eigensolver: a review of methods and best practices. *arXiv preprint arXiv:2111.05176* (2021)
- [23] Grimsley, H.R., Economou, S.E., Barnes, E., Mayhall, N.J.: An adaptive variational algorithm for exact molecular simulations on a quantum computer. *Nature communications* **10**(1), 1–9 (2019)
- [24] Benfenati, F., Mazzola, G., Capecchi, C., Barkoutsos, P.K., Ollitrault, P.J., Tavernelli, I., Guidoni, L.: Improved accuracy on noisy devices by nonunitary variational quantum eigensolver for chemistry applications. *Journal of Chemical Theory and Computation* **17**(7), 3946–3954 (2021)
- [25] Ostaszewski, M., Trenkwalder, L.M., Masarczyk, W., Scerri, E., Dunjko, V.: Reinforcement learning for optimization of variational quantum circuit architectures. *Advances in Neural Information Processing Systems* **34**, 18182–18194 (2021)

- [26] Hong, C.-L., Tsai, T., Chou, J.-P., Chen, P.-J., Tsai, P.-K., Chen, Y.-C., Kuo, E.-J., Srolovitz, D., Hu, A., Cheng, Y.-C., et al.: Accurate and efficient quantum computations of molecular properties using daubechies wavelet molecular orbitals: A benchmark study against experimental data. arXiv preprint arXiv:2205.14476 (2022)
- [27] Verteletskyi, V., Yen, T.-C., Izmaylov, A.F.: Measurement optimization in the variational quantum eigensolver using a minimum clique cover. *The Journal of chemical physics* **152**(12), 124114 (2020)
- [28] Huggins, W.J., McClean, J.R., Rubin, N.C., Jiang, Z., Wiebe, N., Whaley, K.B., Babbush, R.: Efficient and noise resilient measurements for quantum chemistry on near-term quantum computers. *npj Quantum Information* **7**(1), 1–9 (2021)
- [29] Eddins, A., Motta, M., Gujarati, T.P., Bravyi, S., Mezzacapo, A., Hadfield, C., Sheldon, S.: Doubling the size of quantum simulators by entanglement forging. *PRX Quantum* **3**(1), 010309 (2022)
- [30] Bravyi, S., Gambetta, J.M., Mezzacapo, A., Temme, K.: Tapering off qubits to simulate fermionic hamiltonians. arXiv preprint arXiv:1701.08213 (2017)
- [31] Setia, K., Chen, R., Rice, J.E., Mezzacapo, A., Pistoia, M., Whitfield, J.D.: Reducing qubit requirements for quantum simulations using molecular point group symmetries. *Journal of Chemical Theory and Computation* **16**(10), 6091–6097 (2020)
- [32] Berry, D.W., Kieferová, M., Scherer, A., Sanders, Y.R., Low, G.H., Wiebe, N., Gidney, C., Babbush, R.: Improved techniques for preparing eigenstates of fermionic hamiltonians. *npj Quantum Information* **4**(1), 1–7 (2018)
- [33] Schuld, M., Petruccione, F.: *Supervised Learning with Quantum Computers* vol. 17. Springer, [no place] (2018)
- [34] Toloui, B., Love, P.J.: Quantum algorithms for quantum chemistry based on the sparsity of the ci-matrix. arXiv preprint arXiv:1312.2579 (2013)
- [35] Babbush, R., Berry, D.W., Sanders, Y.R., Kivlichan, I.D., Scherer, A., Wei, A.Y., Love, P.J., Aspuru-Guzik, A.: Exponentially more precise quantum simulation of fermions in the configuration interaction representation. *Quantum Science and Technology* **3**(1), 015006 (2017)
- [36] McArdle, S., Mayorov, A., Shan, X., Benjamin, S., Yuan, X.: Digital quantum simulation of molecular vibrations. *Chemical science* **10**(22), 5725–5735 (2019)

- [37] Sawaya, N.P., Menke, T., Kyaw, T.H., Johri, S., Aspuru-Guzik, A., Guerreschi, G.G.: Resource-efficient digital quantum simulation of d-level systems for photonic, vibrational, and spin-s hamiltonians. *npj Quantum Information* **6**(1), 1–13 (2020)
- [38] Di Matteo, O., McCoy, A., Gysbers, P., Miyagi, T., Woloshyn, R., Navrátil, P.: Improving hamiltonian encodings with the gray code. *Physical Review A* **103**(4), 042405 (2021)
- [39] Shee, Y., Tsai, P.-K., Hong, C.-L., Cheng, H.-C., Goan, H.-S.: Qubit-efficient encoding scheme for quantum simulations of electronic structure. *Physical Review Research* **4**(2), 023154 (2022)
- [40] Tubman, N.M., Freeman, C.D., Levine, D.S., Hait, D., Head-Gordon, M., Whaley, K.B.: Modern approaches to exact diagonalization and selected configuration interaction with the adaptive sampling ci method. *Journal of chemical theory and computation* **16**(4), 2139–2159 (2020)
- [41] Bender, C.F., Davidson, E.R.: Studies in configuration interaction: The first-row diatomic hydrides. *Physical Review* **183**(1), 23 (1969)
- [42] Huron, B., Malrieu, J., Rancurel, P.: Iterative perturbation calculations of ground and excited state energies from multiconfigurational zeroth-order wavefunctions. *The Journal of Chemical Physics* **58**(12), 5745–5759 (1973)
- [43] Buenker, R.J., Peyerimhoff, S.D., Butscher, W.: Applicability of the multi-reference double-excitation ci (mrd-ci) method to the calculation of electronic wavefunctions and comparison with related techniques. *Molecular Physics* **35**(3), 771–791 (1978)
- [44] Evangelisti, S., Daudey, J.-P., Malrieu, J.-P.: Convergence of an improved cipsi algorithm. *Chemical Physics* **75**(1), 91–102 (1983)
- [45] Harrison, R.J.: Approximating full configuration interaction with selected configuration interaction and perturbation theory. *The Journal of chemical physics* **94**(7), 5021–5031 (1991)
- [46] Ben Amor, N., Bessac, F., Hoyau, S., Maynau, D.: Direct selected multireference configuration interaction calculations for large systems using localized orbitals. *The Journal of chemical physics* **135**(1), 014101 (2011)
- [47] Giner, E., Scemama, A., Caffarel, M.: Using perturbatively selected configuration interaction in quantum monte carlo calculations. *Canadian Journal of Chemistry* **91**(9), 879–885 (2013)
- [48] Evangelista, F.A.: Adaptive multiconfigurational wave functions. *The*

- Journal of Chemical Physics **140**(12), 124114 (2014)
- [49] Holmes, A.A., Tubman, N.M., Umrigar, C.: Heat-bath configuration interaction: An efficient selected configuration interaction algorithm inspired by heat-bath sampling. *Journal of chemical theory and computation* **12**(8), 3674–3680 (2016)
- [50] Tubman, N.M., Lee, J., Takeshita, T.Y., Head-Gordon, M., Whaley, K.B.: A deterministic alternative to the full configuration interaction quantum monte carlo method. *The Journal of chemical physics* **145**(4), 044112 (2016)
- [51] Zhang, N., Liu, W., Hoffmann, M.R.: Iterative configuration interaction with selection. *Journal of Chemical Theory and Computation* **16**(4), 2296–2316 (2020)
- [52] Pineda Flores, S.D.: Chembot: A machine learning approach to selective configuration interaction. *Journal of Chemical Theory and Computation* **17**(7), 4028–4038 (2021)
- [53] Goings, J.J., Hu, H., Yang, C., Li, X.: Reinforcement learning configuration interaction. *Journal of chemical theory and computation* **17**(9), 5482–5491 (2021)
- [54] Feniou, C., Hassan, M., Traoré, D., Giner, E., Maday, Y., Piquemal, J.-P.: Overlap-adapt-vqe: Practical quantum chemistry on quantum computers via overlap-guided compact ansätze. *arXiv preprint arXiv:2301.10196* (2023)
- [55] Cioabă, S.M., Elzinga, R.J., Gregory, D.A.: Some observations on the smallest adjacency eigenvalue of a graph. *arXiv preprint arXiv:1912.03957* (2019)
- [56] Hehre, W.J., Stewart, R.F., Pople, J.A.: self-consistent molecular-orbital methods. i. use of gaussian expansions of slater-type atomic orbitals. *The Journal of Chemical Physics* **51**(6), 2657–2664 (1969)
- [57] Davidson, E.R.: The iterative calculation of a few of the lowest eigenvalues and corresponding eigenvectors of large real-symmetric matrices. *Journal of Computational Physics* **17**(1), 87–94 (1975). [https://doi.org/10.1016/0021-9991\(75\)90065-0](https://doi.org/10.1016/0021-9991(75)90065-0)
- [58] Bravyi, S.B., Kitaev, A.Y.: Fermionic quantum computation. *Annals of Physics* **298**(1), 210–226 (2002)
- [59] Smith, D.G., Burns, L.A., Simmonett, A.C., Parrish, R.M., Schieber, M.C., Galvelis, R., Kraus, P., Kruse, H., Di Remigio, R., Alenaizan,

- A., *et al.*: Psi4 1.4: Open-source software for high-throughput quantum chemistry. *The Journal of chemical physics* **152**(18), 184108 (2020)
- [60] Du, J., Xu, N., Peng, X., Wang, P., Wu, S., Lu, D.: Nmr implementation of a molecular hydrogen quantum simulation with adiabatic state preparation. *Physical review letters* **104**(3), 030502 (2010)
- [61] Endo, S., Benjamin, S.C., Li, Y.: Practical quantum error mitigation for near-future applications. *Physical Review X* **8**(3), 031027 (2018)
- [62] Powell, M.J.: A direct search optimization method that models the objective and constraint functions by linear interpolation. In: *Advances in Optimization and Numerical Analysis*, pp. 51–67. Springer, Dordrecht (1994)
- [63] Aleksandrowicz, G., Alexander, T., Barkoutsos, P., Bello, L., Ben-Haim, Y., Bucher, D., Cabrera-Hernández, F.J., Carballo-Franquis, J., Chen, A., Chen, C.-F., *et al.*: Qiskit: An open-source framework for quantum computing. Accessed on: Mar **16** (2019)
- [64] Eriksen, J.J., Anderson, T.A., Deustua, J.E., Ghanem, K., Hait, D., Hoffmann, M.R., Lee, S., Levine, D.S., Magoulas, I., Shen, J., *et al.*: The ground state electronic energy of benzene. *The journal of physical chemistry letters* **11**(20), 8922–8929 (2020)
- [65] Lanyon, B.P., Whitfield, J.D., Gillett, G.G., Goggin, M.E., Almeida, M.P., Kassal, I., Biamonte, J.D., Mohseni, M., Powell, B.J., Barbieri, M., *et al.*: Towards quantum chemistry on a quantum computer. *Nature chemistry* **2**(2), 106–111 (2010)
- [66] Jones, M.A., Vallury, H.J., Hill, C.D., Hollenberg, L.C.: Chemistry beyond the hartree–fock energy via quantum computed moments. *Scientific Reports* **12**(1), 1–9 (2022)
- [67] Vallury, H.J., Jones, M.A., Hill, C.D., Hollenberg, L.C.: Quantum computed moments correction to variational estimates. *Quantum* **4**, 373 (2020)
- [68] Meiron, D., Frankel, S.H.: Pansatz: Pulse-based ansatz for variational quantum algorithms. *arXiv preprint arXiv:2212.12911* (2022)
- [69] Fedorov, D.A., Peng, B., Govind, N., Alexeev, Y.: Vqe method: A short survey and recent developments. *Materials Theory* **6**(1), 1–21 (2022)
- [70] Johnson III, R.D., *et al.*: Nist 101. computational chemistry comparison and benchmark database (1999)

- [71] Gokhale, P., Angiuli, O., Ding, Y., Gui, K., Tomesh, T., Suchara, M., Martonosi, M., Chong, F.T.: Minimizing state preparations in variational quantum eigensolver by partitioning into commuting families. arXiv preprint arXiv:1907.13623 (2019)
- [72] Garniron, Y.: Development and parallel implementation of selected configuration interaction methods. PhD thesis, Université Paul Sabatier-Toulouse III (2018)
- [73] Vogiatzis, K.D., Ma, D., Olsen, J., Gagliardi, L., De Jong, W.A.: Pushing configuration-interaction to the limit: Towards massively parallel mscf calculations. *The Journal of chemical physics* **147**(18), 184111 (2017)